

Single Chain-Crosslinked Star Polymers via Intramolecular Crosslinking of Self-Folding Amphiphilic Copolymers in Water

Takaya Terashima,* Takanori Sugita, Mitsuo Sawamoto*

*Corresponding Author

Department of Polymer Chemistry, Graduate School of Engineering, Kyoto University

Katsura, Nishikyo-ku, Kyoto 615-8510, JAPAN

Tel: +81-75-383-2600, Fax: +81-75-383-2601

E-mail: terashima@living.polym.kyoto-u.ac.jp, sawamoto@star.polym.kyoto-u.ac.jp

Abstract

Single-chain crosslinked star polymers with hydrophilic multiple short arms and a hydrophobic core were created as novel microgel star polymers of single polymer chains. The synthetic process involves the intramolecular crosslinking of self-folding amphiphilic random copolymers in water. For this, amphiphilic random copolymers bearing hydrophilic poly(ethylene glycol) (PEG) and hydrophobic olefin pendants were synthesized by ruthenium-catalyzed living radical copolymerization of PEG methyl ether methacrylate, dodecyl methacrylate, and hydroxyl-functionalized methacrylates, and the in-situ or post esterification of the hydroxyl pendants of the resulting copolymers with methacryloyl chloride. The olefin-bearing copolymers with 20-40 mol% hydrophobic units efficiently self-folded with hydrophobic interaction in water and were crosslinked intramolecularly using a free radical initiator or a ruthenium catalyst to selectively provide single-chain crosslinked star polymers, while a counterpart with 50 mol% hydrophobic units induced bimolecular aggregation in water to give double-chain crosslinked star polymers. Primary structure of the star polymers can be precisely controlled with random copolymer precursors. Owing to PEG arm units, the star polymers further showed thermosensitive solubility in water.

Keyword

Star polymer, amphiphilic copolymer, single-chain polymeric nanoparticle, folding, crosslinking, hydrophobic interaction

Running Head

Single chain-crosslinked star polymers

Introduction

Local crosslinking of polymer chains and their aggregates is a key technology to build soluble functional macromolecules of stable three-dimensional architecture in various solvents and environments.¹⁻⁵ Microgel-core star polymers^{1-4,6-12} are representative core-shell macromolecules carrying a microgel core that is covered by multiple linear arm polymers. The crosslinked core not only serves to maintain the star-branched structure in various environments but also provides unique nano compartments for catalysis⁸⁻¹¹ and molecular encapsulation and release.¹² Such functionalized star polymers are efficiently obtained via the local crosslinking of living linear polymers (or macroinitiators) with functional linking agents (e.g., divinyl compounds) and monomers in living radical polymerization.¹³ However, microgel-core star polymers in principle involve difficulty on the on-demand control of the numbers of arm chains and in-core functionality because the core-forming process (micro-gelation) competitively undergoes both “intermolecular” and “intramolecular” crosslinking of multiple polymer chains; the crosslinking efficiency thus depends on the total concentration of arm polymers ($[\text{arm}]_0$) and monomers ($[\text{linker}]_0$, $[\text{monomer}]_0$) in addition to the molar ratio of monomers to arm chains ($[\text{linker}]_0/[\text{monomer}]_0/[\text{arm}]_0$).

In contrast, single-chain folding polymers, single-chain polymeric nanoparticles (SCPNs), and unimer micelles literally comprise single polymer chains that self-fold with “intramolecular” physical association and/or covalent linking in solutions.¹⁴⁻³⁵ They can thus provide functional nanospaces based on single polymer chains.^{17,18,25,27} Recently, we have synthesized various amphiphilic and functional random copolymers via living radical polymerization to create single-chain folding (self-folding) polymers with hydrophobic and hydrogen-bonding interactions in water.²³⁻²⁷ Compared with conventional microgel-core star polymers, single-chain folding polymers have several inherent features: 1) the primary structure (e.g., molecular weight, monomer composition and sequence, and terminal structure and number) of single-chain folding polymers is identical to that of random copolymer precursors; 2) folding properties are tunable by monomer composition, monomer species, and degree of polymerization; and 3) folding structure is dynamically and reversibly variable by external stimuli.

For instance, PEGMA/DMA amphiphilic random copolymers of hydrophilic poly(ethylene glycol) chains and hydrophobic dodecyl pendants [PEGMA: $\text{CH}_2=\text{CMeCO}_2(\text{CH}_2\text{CH}_2\text{O})_{8.5}\text{CH}_3$, $M_n = 475$, DMA: dodecyl ($-\text{C}_{12}\text{H}_{25}$) methacrylate] showed unique self-folding and aggregation properties in water through DMA content control: the copolymers with 20 - 40 mol% DMA selectively form self-folding unimer micelles with hydrophobic interaction in water, while that with 50 mol% DMA in turn forms a double chain aggregate in water.²³ Such self-folding polymers have dynamic and hydrophobic cores of polymethacrylate backbones and dodecyl pendants that are stabilized by

multiple short PEG chains. They are thus structurally regarded as single-chain dynamic star polymers. With these intriguing features, PEGMA/DMA-based copolymers would be one of the most promising scaffolds for precisely functionalized nanospaces, whereas the folding structure is formed just in water and easily varied into unfolded (random coil) structure in organic solvents.

We herein produced single-chain crosslinked star polymers via the intramolecular crosslinking (patching) of self-folding amphiphilic random copolymers in water (Scheme 1). This is a new class of microgel star polymers, where the number of arms and functionality, and the crosslinking density are efficiently and directly controlled with random copolymer precursors that are prepared by living radical polymerization. Single-chain crosslinked star polymers can further maintain compact folding structure even in organic solvents.

Scheme 1

Single-chain crosslinked star polymers were prepared via the four steps: 1) polymerization, 2) pendant-olefin introduction, 3) single-chain folding, and 4) intramolecular crosslinking. Hydroxyl-functionalized amphiphilic random copolymers (**P1-P7**) were first synthesized by living radical copolymerization of PEGMA, DMA, and hydroxyl-functionalized monomers [12-hydroxydodecyl methacrylate (HDMA) or 2-hydroxyethyl methacrylate (HEMA)]. The composition of hydrophobic monomers (DMA, HDMA) was precisely controlled: 20, 40, and 50 mol% per a chain. The hydroxyl-functionalized copolymers were then quantitatively esterified with methacryloyl chloride (MAC) to give olefin-bearing amphiphilic random copolymers (**P1-O-P7-O**). **P1-O-P7-O** underwent self-folding or double-chain aggregation with hydrophobic interaction in water and then homogeneously crosslinked with a free radical initiator or a ruthenium catalyst to give star polymers (**S1-S7**). The selective intramolecular crosslinking without macroscopic gelation was attributed to the local accumulation of hydrophobic olefin pendants into the central cores and the efficient isolation of their polymer chains by multiple hydrophilic PEG chains.

Experimental Section

Materials. For polymerization, poly(ethylene glycol) methyl ether methacrylate [PEGMA; $\text{CH}_2=\text{CMeCO}_2(\text{CH}_2\text{CH}_2\text{O})_{8.5}\text{Me}$; $M_n = 475$] (Aldrich, St Louis, MO, USA) and dodecyl methacrylate (DMA) (Wako, Osaka, Japan, purity >95%) were purified by column chromatography charged with inhibitor remover (Aldrich) and degassed by triple vacuum-argon purge cycles before use. 2-Hydroxyethyl methacrylate (HEMA: Aldrich; purity >99%), ethyl 2-bromoisobutyrate (**1**, TCI, Tokyo, Japan, purity >98%), and ethyl 2-chloro-2-phenylacetate (**4**: Aldrich, purity >97%) were distilled under reduced pressure before use. 12-Hydroxydodecyl methacrylate (HDMA), a bifunctional initiator (**2**), and a trifunctional initiator (**3**) were synthesized as shown below. Methacryloyl chloride (MAC: TCI; purity >80.0%) and triethylamine (TCI, purity >99.0%) were purified by distillation before use. 1,12-Dodecanediol (Aldrich, purity >99%), 2-bromo-2-methylpropanoyl bromide (Aldrich, purity >98%), 1,4-bis(2-hydroxyethoxy)benzene (TCI, purity >95%), and 1,1,1-tris(hydroxymethyl)ethane (Aldrich, purity >99%) were degassed by triple vacuum-argon purge cycles before use. $\text{Ru}(\text{Ind})\text{Cl}(\text{PPh}_3)_2$ (Aldrich), $\text{RuCp}^*\text{Cl}(\text{PPh}_3)_2$ (Cp^* : pentamethylcyclopentadienyl, Aldrich, purity >97%), and (4-hydroxyphenyl)diphenylphosphine [$\text{PPh}_2(\text{C}_6\text{H}_4\text{OH})$: Aldrich, purity >98%]³⁶ were used as received, and $[\text{RuCp}^*(\mu_3\text{-Cl})]_4$ was synthesized according to the published procedure.³⁷ These ruthenium complexes and a ligand were handled in a glove box under moisture- and oxygen-free argon ($\text{H}_2\text{O} < 1 \text{ ppm}$; $\text{O}_2 < 1 \text{ ppm}$). 1,2,3,4-tetrahydronaphthalene (tetralin, Kisida Chemical, Osaka, Japan, purity >98%), an internal standard for monomer conversion determined by ^1H NMR, was dried over calcium chloride overnight and distilled twice from calcium hydride. $n\text{-Bu}_3\text{N}$ (Tokyo Kasei, purity >99%), 4-dimethylamino-1-butanol (4-DMAB: TCI, purity >98%),³⁸ 2,2'-azobis(2-methylpropionamide) dihydrochloride (V-50: Wako, purity >95%), dimethyl 2,2'-azobis(isobutyrate) (MAIB: Wako, purity >97%), ethanol (Wako, dehydrated), and pure water (Wako) were degassed before use. Toluene was purified before use; passing it through a purification column (Glass Contour Solvent Systems: SG Water USA, NH, USA). Dry THF (Wako, dehydrated) and dry diethyl ether (Wako, purity >99.5%) were used without further purification.

Characterization. The molecular weight distribution (MWD) curves, number-average molecular weight (M_n), peak top molecular weight (M_p), and M_w/M_n ratio of polymers were measured by SEC in DMF containing 10 mM LiBr at 40 °C (flow rate: 1 mL/min) on three linear-type polystyrene gel columns (KF-805L, Shodex, Tokyo, Japan: exclusion limit = 4×10^6 mol/g, particle size = 10 μm , pore size = 5000 Å, 0.8 cm i.d. \times 30 cm) that were connected to a Jasco PU-2080 precision pump, a Jasco RI-2031 refractive index detector, and a Jasco UV-2075 UV/vis detector set at 270 nm (Jasco,

Tokyo, Japan). The columns were calibrated against 10 standard poly(MMA) samples (Polymer Laboratories, Church Stretton, UK, $M_n = 1000\text{--}1200000$ g/mol, $M_w/M_n = 1.06\text{--}1.22$). ^1H NMR spectra were recorded in CDCl_3 , acetone- d_6 , DMF- d_7 , and D_2O on a JEOL JNM-ECA500 spectrometer operating at 500.16 MHz (JEOL, Tokyo, Japan). Electrospray ionization mass spectrometry (ESI-MS) was performed on Waters Quattro micro API (Waters, Milford, MA, USA). Absolute weight-average molecular weight (M_w) in DMF was determined by multi-angle laser light scattering (MALLS) equipped with SEC on a Dawn E instrument (Wyatt Technology; Santa Barbara, CA, USA; Ga-As laser; $\lambda = 690$ nm). The SEC was performed in DMF containing 10 mM LiBr at 40 °C (flow rate: 1 mL/min) on three linear-type polystyrene gel columns (Shodex KF-805L) that were connected to a Jasco PU-2080 precision pump, a Jasco RI-1530 refractive index detector, and a Jasco UV-1570 UV/vis detector set at 270 nm. Refractive index increment (dn/dc) was measured in DMF at 40 °C on an Optilab DSP refractometer (Wyatt Technology; $\lambda = 690$ nm, $c < 2.5$ mg/mL). Dynamic light scattering (DLS) was measured on Otsuka Photal ELSZ-0 equipped with a semi-conductor laser (wavelength: 658 nm) at 25 °C (Otsuka, Osaka, Japan). The measuring angle was 165° and the data was analyzed by CONTIN method. Ultraviolet-visible (UV/Vis) spectra were obtained from Shimadzu MultiSpec-1500 or UV-1800 in H_2O /acetone (19/1) and acetone at 25 °C (optical path length = 1.0 cm) (Shimadzu, Kyoto, Japan). TEM images were taken by using a JEOL JEM-2000EXII at an acceleration voltage of 100 kV. The aqueous solutions of polymers were applied to a carbon-coated Cu grid, and the samples were negatively stained with 2% uranyl acetate, followed by suctioning the excess fluid with filter paper.

Synthesis of HDMA. In 100 mL round-bottomed flask filled with argon, MAC (18.6 mmol, 1.8 mL) was slowly added to the solution of 1,12-dodecanediol (27.9 mmol, 5.6 g) and triethylamine (20.8 mmol, 2.9 mL) in dry THF (25 mL) at r.t.. The reaction mixture was stirred at 25 °C for 18 h. After the evaporation, diethyl ether (50 mL) and distilled water (50 mL) were poured into the crude. The aqueous phase was separated and extracted by diethyl ether (50 mL), and the ether extracts were combined with the organic layer. The combined organic phase was washed with water three times, ammonia water, and brine, and was dried over anhydrous Na_2SO_4 overnight. After the ether was removed in vacuo, the crude product was purified by silica gel column chromatography with hexane/ethyl acetate (80/20, v/v) to give HDMA as a colorless liquid (0.98 g, 20% yield). ^1H NMR [500 MHz, CDCl_3 , 25 °C, $\delta = 0$ TMS] $\delta = 6.08$ (s, 1 H), 5.45 (m, 1 H), 4.09 (t, 2 H, $J = 6.7$ Hz), 3.50 (t, 2 H, $J = 6.7$ Hz), 1.90 (s, 3 H), 1.61 (quin, 2 H, $J = 6.7$ Hz), 1.47 (quin, 2 H, $J = 6.7$ Hz), 1.35 - 1.22 (16 H). ^{13}C NMR [125 MHz, CDCl_3 , 25 °C, $\delta = 77.0$ CDCl_3] $\delta = 167.4$, 136.4, 125.2, 64.7, 62.7, 32.6, 29.5-29.3, 29.1, 28.5, 25.8, 25.6, 18.2. ESI-MS m/z ($[\text{M} + \text{Na}]^+$) calcd. for $\text{C}_{12}\text{H}_{22}\text{O}_2\text{Na}$ 221.2, found 221.4.

Synthesis of a bifunctional initiator (2). In 100 mL round-bottomed flask filled with argon, 2-bromo-2-methylpropanoyl bromide (6.5 mmol, 0.80 mL) was added to the solution of 1,4-bis(2-hydroxyethoxy)benzene (1.8 mmol, 0.35 g) and triethylamine (6.5 mmol, 0.91 mL) in dry THF (20 mL) at 0 °C. The reaction mixture was stirred at 25 °C for 18 h. After the evaporation of the reaction solution, diethyl ether (50 mL) and distilled water (50 mL) were poured into the flask. The aqueous phase was separated and extracted by diethyl ether (50 mL), and the ether extracts were combined with the organic layer. The combined organic phase was washed with water three times, ammonia water, and brine, and was dried over anhydrous Na₂SO₄ overnight. After the ether was removed in vacuo, a pure solid product (bifunctional initiator: **2**) was obtained (0.72 g, 80% yield). ¹H NMR [500 MHz, CDCl₃, 25 °C, δ = 7.26 (CHCl₃)] δ = 6.86 (s, 4H), 4.49 (t, 4H, *J* = 5.3 Hz), 4.17 (t, 4H, *J* = 4.8 Hz), 1.93 (s, 12H). ¹³C NMR [125 MHz, CDCl₃, 25 °C, δ = 77.0 (CDCl₃)] δ = 171.6, 153.1, 115.9, 66.4, 64.3, 55.5, 30.7.

Synthesis of a trifunctional initiator (3). In 100 mL round-bottomed flask filled with argon, 2-bromo-2-methylpropanoyl bromide (16 mmol, 1.98 mL) was added to the solution of 1,1,1-tris(hydroxymethyl)ethane (3.5 mmol, 0.42 g) and triethylamine (16 mmol, 2.2 mL) in dry THF (60 mL) at 0 °C. The reaction mixture was stirred at 25 °C for 18 h. After the evaporation of the reaction solution, diethyl ether (50 mL) and distilled water (50 mL) were poured into the flask. The aqueous phase was separated and extracted by diethyl ether (50 mL), and the ether extracts were combined with the organic layer. The combined organic phase was washed with water three times, ammonia water, and brine, and was dried over anhydrous Na₂SO₄ overnight. After the ether was removed in vacuo, a pure solid product [1,1,1-tris(2-bromoisobutyryloxymethyl)ethane: **3**] was obtained (0.99 g, 50% yield). ¹H NMR [500 MHz, CDCl₃, 25 °C, δ = 7.26 (CHCl₃)] δ = 4.12 (s, 6H), 1.94 (s, 18H), 1.17 (s, 3H). ¹³C NMR [125 MHz, CDCl₃, 25 °C, δ = 77.0 (CDCl₃)] δ = 171.2, 66.6, 55.4, 39.7, 30.7, 16.9.

Synthesis of Olefin-Bearing Amphiphilic Copolymers

The synthesis of olefin-bearing amphiphilic copolymers (**P1-O** – **P7-O**) was carried out by syringe technique under argon in baked glass flasks or tubes equipped with a three-way stopcock via ruthenium-catalyzed living radical polymerization and the post- or in situ esterification of hydroxyl-bearing copolymers with MAC.

P2-O (via in situ esterification): In 30 mL glass tube, Ru(Ind)Cl(PPh₃)₂ (0.008 mmol, 6.4 mg) was placed. Then, THF (4.6 mL), tetralin (0.1 mL), a 400 mM THF solution of *n*-Bu₃N (0.4 mL, *n*-Bu₃N = 0.16 mmol), PEGMA (2.4 mmol, 1.1 mL), DMA (1.2 mmol, 0.35 mL), a 308 mM THF

solution of HDMA (1.3 mL, HDMA = 0.4 mmol), and a 143 mM THF solution of **2** (0.11 mL, **2** = 0.016 mmol) were added sequentially in that order into the tube at 25 °C under argon. The total volume of the reaction mixture was thus 8.0 mL. The tube was placed in an oil bath kept at 60 °C. At predetermined intervals, the mixture was sampled with a syringe under dry argon, and the reaction was terminated by cooling the solution to -78 °C. After 25 h, the conversion of PEGMA/DMA+HDMA reached 80%/80%, respectively, determined by ¹H NMR with tetralin as an internal standard. Into this solution, MAC (0.19 mL, 2 mmol) was directly added at 0 °C. The mixture was stirred for 16 h at 25 °C. Then, the reaction was quenched with dry ethanol (5 mL). After the solvent was removed in vacuo, the crude polymer was purified by silica gel column chromatography with toluene as an eluent and precipitated into hexane to give **P2-O**. SEC (DMF, PMMA std.): $M_n = 58500$ g/mol; $M_w/M_n = 1.27$. SEC-MALLS (DMF, 0.01 M LiBr): $M_w = 126000$ g/mol. ¹H NMR [500 MHz, acetone-*d*₆, 25 °C, $\delta = 2.04$ (CD₂HCOCD₃)]: δ 6.95–6.85 (aromatic), 6.09–6.04 (olefin), 5.65–5.60 (olefin), 4.25–4.06 (-COOCH₂CH₂O-, CH₂=C(CH₃)COOCH₂CH₂CH₂-), 4.06–3.90 (-COOCH₂CH₂CH₂-), 3.81–3.43 (-OCH₂CH₂O-), 3.36–3.28 (-OCH₃), 2.16–1.78 (-CH₂C(CH₃)-), 1.93 (CH₂=C(CH₃)COO-), 1.74–1.63 (-COOCH₂CH₂(CH₂)₉CH₃), 1.53–1.27 (-COOCH₂CH₂(CH₂)₉CH₃), 1.17–0.85 (-COO(CH₂)₁₁CH₃, -CH₂C(CH₃)-); PEGMA/DMA/HEMA-olefin = 157/76/23; M_n (NMR, *a*) = 102000. **P3-O**, **P4-O**, and **P5-O** were similarly synthesized.

P7-O (via post-esterification): In 100 mL round-bottom flask, RuCp*Cl(PPh₃)₂ (0.0075 mmol, 6.0 mg) was placed. Then, ethanol (29 mL), tetralin (0.5 mL), a 400 mM toluene solution of 4-DMAB (2 mL, 4-DMAB = 0.8 mmol), PEGMA (16 mmol, 7.0 mL), DMA (4.0 mmol, 1.2 mL), HEMA (1.0 mmol, 0.12 mL), and a 486 mM toluene solution of ECPA (0.16 mL, ECPA = 0.08 mmol) were added sequentially in that order into the tube at 25 °C under argon. The total volume of the reaction mixture was thus 40 mL. The flask was placed in an oil bath kept at 40 °C. At predetermined intervals, the mixture was sampled with a syringe under dry argon, and the reaction was terminated by cooling the solution to -78 °C. After 47 h, the conversion of PEGMA/DMA/HEMA reached 74%/78%/80%, respectively, determined by ¹H NMR with tetralin as an internal standard. The quenched solution was evaporated to dryness. The crude polymer was purified by silica gel column chromatography with toluene as an eluent and precipitated into hexane to give **P7**. SEC (DMF, PMMA std.): $M_n = 57000$ g/mol; $M_w/M_n = 1.20$.

In 100 mL round-bottom flask filled with argon, MAC (5.0 mmol, 0.48 mL) was added to the solution of **P7** (5.6 g, [OH] = ~1 mmol) and triethylamine (6.0 mmol, 0.83 mL) in dry THF (20 mL) at 0 °C. The reaction mixture was stirred at 25 °C for 18 h. Then, the reaction was quenched with dry ethanol (5 mL). After the solvent was removed in vacuo, the crude product was purified

by silica gel column chromatography with toluene as an eluent and precipitated into hexane to give **P7-O**. SEC (DMF, PMMA std.): $M_n = 58800$ g/mol; $M_w/M_n = 1.18$. SEC-MALLS (DMF, 0.01 M LiBr): $M_w = 109000$ g/mol. $^1\text{H NMR}$ [500 MHz, CD_3OD , 25 °C, $\delta = 3.30$ (CD_2HOD)]: δ 7.35–7.20 (aromatic), 6.21–6.16 (olefin), 5.77–5.70 (olefin), 4.46–4.20 (- $\text{COOCH}_2\text{CH}_2\text{OCO}$ -), 4.18–4.05 (- $\text{COOCH}_2\text{CH}_2\text{O}$ -), 4.05–3.90 (- $\text{COOCH}_2\text{CH}_2\text{CH}_2$ -), 3.82–3.47 (- $\text{OCH}_2\text{CH}_2\text{O}$ -), 3.39–3.35 (- OCH_3), 2.00 ($\text{CH}_2=\text{C}(\text{CH}_3)\text{COO}$ -), 2.20–1.75 (- $\text{CH}_2\text{C}(\text{CH}_3)$ -), 1.75–1.60 (- $\text{COOCH}_2\text{CH}_2(\text{CH}_2)_9\text{CH}_3$), 1.58–1.20 (- $\text{COOCH}_2\text{CH}_2(\text{CH}_2)_9\text{CH}_3$), 1.20–0.70 (- $\text{COO}(\text{CH}_2)_{11}\text{CH}_3$, - $\text{CH}_2\text{C}(\text{CH}_3)$ -); PEGMA/DMA/HEMA-olefin = 141/35/8.3; M_n (NMR, *a*) = 77000. **P1-O** and **P6-O** were similarly synthesized.

Intramolecular Crosslinking of Olefin-Bearing Amphiphilic Copolymers in Water

The synthesis of star polymers (**S1-S7**) was carried out by syringe technique under argon in baked glass tubes or flasks equipped with a three-way stopcock.

S2 (with a ruthenium catalyst): In a 30 mL glass tube, $[\text{RuCp}^*\text{Cl}]_4$ (0.43 mg, 0.0004 mmol) and $\text{PPh}_2(\text{C}_6\text{H}_4\text{OH})$ (0.89 mg, 0.0032 mmol) were mixed in toluene (0.72 mL) at 80 °C for 12 h under argon. The solution was then evaporated in vacuo at 25 °C to give a solid ruthenium complex. Into the tube, the ethanol solution of **P2-O** (90 mg/mL, 0.4 mL, **P2-O** = 36 mg, olefin = 0.008 mmol), ethanol (0.4 mL), and H_2O (7.2 mL) were added at 25 °C under argon. The mixture was kept at 25 °C and sampled with a syringe at predetermined periods to determine the conversion of the olefin by $^1\text{H NMR}$ (63% conversion in 120 h). After the solution was evaporated in vacuo in the presence of toluene, the crude product was purified by silica gel column chromatography with toluene as an eluent and precipitated into hexane to give **S2**. SEC (DMF, PMMA std.): $M_n = 48900$ g/mol; $M_w/M_n = 1.22$. SEC-MALLS (DMF, 0.01 M LiBr): $M_w = 120000$ g/mol. $^1\text{H NMR}$ [500 MHz, CDCl_3 , 25 °C, $\delta = 7.26$ (CHCl_3)]: δ 6.10–6.09 (olefin), 5.55–5.53 (olefin), 4.17–4.0 (- $\text{COOCH}_2\text{CH}_2\text{O}$ -), 4.0–3.82 (- $\text{COOCH}_2\text{CH}_2\text{CH}_2$ -), 3.72–3.46 (- $\text{OCH}_2\text{CH}_2\text{O}$ -), 3.39–3.34 (- OCH_3), 2.13–1.70 (- $\text{CH}_2\text{C}(\text{CH}_3)$ -), 1.70–1.55 (- $\text{COOCH}_2\text{CH}_2(\text{CH}_2)_9\text{CH}_3$), 1.45–1.20 (- $\text{COOCH}_2\text{CH}_2(\text{CH}_2)_9\text{CH}_3$), 1.18–0.70 (- $\text{COO}(\text{CH}_2)_{11}\text{CH}_3$, - $\text{CH}_2\text{C}(\text{CH}_3)$ -). **S1**, **S3-S5** were similarly synthesized with their corresponding copolymers.

S7 (with a free radical initiator): In a 100 mL round bottom flask, **P7-O** (250 mg, olefin = 0.027 mmol), V-50 (25 mg, 0.092 mmol) and H_2O (25 mL) were added at 25 °C under argon (total volume: 25 mL). The mixture was kept at 25 °C under UV irradiation (375 nm) for 72 h (77% conversion: determined by $^1\text{H NMR}$). After the water was removed in vacuo in the presence of toluene, the crude product was purified by silica gel column chromatography with toluene as an eluent and precipitated into hexane to give **S7**. SEC (DMF, PMMA std.): $M_n = 50200$ g/mol; $M_w/M_n = 1.23$. SEC-MALLS (DMF, 0.01 M LiBr): $M_w = 118000$ g/mol. $^1\text{H NMR}$ [500 MHz,

DMF-*d*₇, 25 °C, δ = 8.01 (DMF)]: δ 7.41–7.25 (aromatic), 6.22–6.15 (olefin), 5.86–5.75 (olefin), 4.55–4.26 (-COOCH₂CH₂OCO-), 4.26–4.07 (-COOCH₂CH₂O-), 4.07–3.93 (-COOCH₂CH₂CH₂-), 3.85–3.40 (-OCH₂CH₂O-), 3.39–3.26 (-OCH₃), 2.30–1.77 (-CH₂C(CH₃)-), 1.77–1.63 (-COOCH₂CH₂(CH₂)₉CH₃), 1.60–1.27 (-COOCH₂CH₂(CH₂)₉CH₃), 1.21–0.70 (-COO(CH₂)₁₁CH₃, -CH₂C(CH₃)-). **S6** was similarly obtained with **S6-O** and V-50.

Results and Discussion

Design of Olefin-Bearing Amphiphilic Random Copolymers

Olefin-bearing amphiphilic random copolymers (**P1-O-P7-O**) were synthesized as precursors for star polymers (**S1-S7**) via the two steps: 1) preparation of hydroxyl-functionalized amphiphilic random copolymers (**P1-P7**) via ruthenium-catalyzed living radical copolymerization; 2) introduction of methacrylate units into **P1-P7** via the in-situ or post-esterification of the hydroxyl pendants with methacryloyl chloride (MAC) (Scheme 1). Hydrophilic poly(ethylene glycol) (PEG: $-(\text{CH}_2\text{CH}_2\text{O})_{8.5}\text{Me}$) and hydrophobic dodecyl groups ($-\text{C}_{12}\text{H}_{24}-$ or $-\text{C}_{12}\text{H}_{25}$) were introduced into the side chains of **P1-P7** in order to induce the efficient self-folding and/or association of corresponding **P1-O-P7-O** in water.

Polymerization. **P1-P7** were synthesized by ruthenium-catalyzed copolymerization of poly(ethylene glycol) methyl ether methacrylate (PEGMA: $M_n = 475$), dodecyl methacrylate (DMA), and 12-hydroxydodecyl methacrylate (HDMA) or 2-hydroxyethyl methacrylate (HEMA) with alkyl halide initiators (**1-4**) (Table 1). Here, three kinds of catalytic systems were employed: $\text{Ru}(\text{Ind})\text{Cl}(\text{PPh}_3)_2/n\text{-Bu}_3\text{N}$ in THF at 60 °C (**P2-P5**), $\text{Ru}(\text{Ind})\text{Cl}(\text{PPh}_3)_2/n\text{-Bu}_3\text{N}$ in toluene at 80 °C (**P6**), and $\text{RuCp}^*\text{Cl}(\text{PPh}_3)_2/4\text{-dimethylamino-1-butanol}$ (4-DMAB) in ethanol at 40 °C (**P1, P7**). The $\text{Ru}(\text{Ind})\text{Cl}(\text{PPh}_3)_2/n\text{-Bu}_3\text{N}$ system with THF allowed us to directly prepare olefin-bearing copolymers (**P2-O – P5-O**) by the in-situ esterification of generating copolymers (**P2 - P5**) via the sequential addition of MAC without any isolation. HDMA in **P1-P6** served as a hydrophobic monomer that placed olefin far from the methacrylate backbones via a long dodecyl linkage ($-\text{C}_{12}\text{H}_{24}-$), while HEMA in **P7** gave olefin close to the polymer backbone via a short ethylene spacer ($-\text{C}_2\text{H}_4-$). In addition to monofunctional bromide or chloride initiators (**1, 4**), dibromide (**2**) or tribromide (**3**) initiators²⁴ were employed to investigate the effects of active terminal numbers and branched structures on the single-chain crosslinking properties (discussed later). The following parameters were systematically varied: the feed ratio of monomers to an initiator ($l = [\text{PEGMA}]_0/[\text{initiator}]_0$, $m = [\text{DMA}]_0/[\text{initiator}]_0$, $n = [\text{HDMA or HEMA}]_0/[\text{initiator}]_0$); the total degree of polymerization ($DP = l + m + n = 200$ (**P1**), 250 (**P2-P6**), 263 (**P7**)); the molar ratio of their hydrophobic monomers [$100 \times (m + n)/DP$] = 20 (**P6, P7**), 40 (**P1-P4**), 50 (**P5**) mol%; the molar ratio of hydroxyl-functionalized monomers for crosslinking units [$100 \times n/DP$] = 5 (**P7**), 10 (**P1-P3, P5**), 20 (**P6**), 40 (**P4**) mol%.

Table 1

As typically shown in Figure 1, all copolymerization smoothly proceeded via the simultaneous consumption of monomers up to 74-93% conversion, independently of ruthenium catalysts, initiators, monomers, and solvents, to provide hydroxyl-functionalized copolymers with controlled molecular weight and narrow molecular weight distribution (**P1-P7**, $M_n = 47400 - 73600$, $M_w/M_n = 1.2 - 1.4$, determined by SEC in DMF with PMMA std. calibration, Table 1).

Figure 1

Pendant-olefin introduction. Esterification of the hydroxyl pendants of **P1 - P7** was examined with MAC in the presence of triethylamine in THF at 25 °C ($[OH]_0/[MAC]_0 = 1/5$). **P1**, **P6**, and **P7** were isolated by preparative SEC (the removal of ruthenium catalysts and monomers) and then esterified with MAC, whereas **P2-P5** were sequentially esterified via the direct addition of MAC into polymerization solutions. After mixing their solutions for 16 – 18 h, the products were analyzed by 1H NMR in acetone- d_6 or methanol- d_4 .

Figure 2

As typically shown in Figure 2, **P1-O - P7-O** exhibited proton signals of olefin (n : 6.2 – 6.1, 5.7 – 5.6 ppm) and methyl groups (o : 2.0 – 1.9 ppm) of the pendant methacrylates, in addition to those of PEG units (c : 4.2 – 4.1 ppm, d : 3.8 – 3.4 ppm, e : 3.4 – 3.3 ppm), dodecyl pendants ($-C_{12}H_{25}$ or $-C_{12}H_{24}$, f, j : 4.1 – 3.9 ppm, g, k : 1.7 ppm, h, l : 1.5 – 1.3 ppm, i : 1.0 – 0.7 ppm), ethyl pendants ($-C_2H_4$, j' : 4.5 – 4.1 ppm), and methacrylate backbones (a : 1.2 – 0.7 ppm, b : 2.2 – 1.8 ppm). Confirmed by the peak area ratio of the pendant olefin (n) to respective monomer units [PEGMA (c, e), DMA (f), HDMA or HEMA (j)], **P1-P7** were almost quantitatively esterified with MAC into **P1-O - P7-O**. It should be noted that in-situ esterification was as effective as post-counterpart. **P2-O, P4-O - P7-O** further exhibited aromatic proton signals (p) derived from the initiating sites of **2** (~6.9 ppm) or **4** (7.3 – 7.2 ppm) (Figure 2c,d). Estimated from the peak area ratio of the monomer units to the initiators (p), DP of respective monomers ($l/m/n_{DP}$) was close to DP calculated from their feed ratios ($l/m/n_{calcd}$) (Table 2). The number average molecular weight for **P2-O, P4-O - P7-O** [M_n (NMR)] was thus determined as 77700 - 107000 by 1H NMR.

Table 2

After esterification, **P1-O - P7-O** still maintain narrow molecular weight distribution ($M_w/M_n = 1.2 - 1.4$) and number-average molecular weight almost identical to the precursors (**P1 - P7**)

(Figure 1, Table 2). The absolute weight-average molecular weight ($M_{w,O}$) was determined by multi-angle laser light scattering coupled with SEC (SEC-MALLS): $M_{w,O} = 109000 - 160000$. $M_{w,O}$'s for **P2-O**, **P4-O** – **P7-O** were in good agreement with the values calculated from M_n (NMR) and M_w/M_n [M_n (NMR) \times M_w/M_n].

Intramolecular Crosslinking of Self-Folding Copolymers in Water

PEGMA/DMA random copolymers with 20 - 40 mol% hydrophobic DMA units efficiently self-fold in water with hydrophobic interaction.²³ Prior to the intramolecular crosslinking, self-folding properties of **P7-O** (19 mol% DMA) in water were investigated by dynamic light scattering (DLS). As expected, hydrodynamic radius of **P7-O** in water ($R_h = 6.4$ nm) was smaller than that in CH_2Cl_2 (8.5 nm), indicating that **P7-O** self-folds in water to form unimer micelle that locally accumulates hydrophobic pendants within the interior. Given these features, we examined the synthesis of single-chain crosslinked star polymers in water via the two strategies: 1) free radical crosslinking with an azo initiator; 2) living radical crosslinking from a polymer terminal with a ruthenium catalyst (Scheme 1, Table 3).

Table 3

Free radical crosslinking. The intramolecular crosslinking of **P6-O** or **P7-O** was investigated with a water-soluble azo initiator [2,2'-azobis(2-methylpropionamide) dihydrochloride: V-50] in water under UV irradiation (375 nm) at 25 °C ($[\text{polymer}]_0 = 10$ mg/mL, Figure 3, Table 3). **P6-O** and **P7-O** possess comparable hydrophobicity (~20 mol% HDMA or DMA), whereas the olefin content and position are different: **P6-O** contains 20 mol% olefin (per total DP) dangling via a dodecyl (HDMA) spacer, while **P7-O** has 5 mol% olefin via an ethylene (HEMA) spacer. Both crosslinking reactions homogeneously proceeded without any macroscopic gelation up to 89% olefin conversion in 16 h (**P6-O**) and 77% in 72 h (**P7-O**) (confirmed by ^1H NMR) to provide **S6** and **S7** with narrow molecular weight distribution ($M_w/M_n = 1.2 - 1.3$, by SEC in DMF, Figure 3a, 3c). Importantly, M_n 's of **S6** and **S7** by SEC were smaller than those of the corresponding precursors (**P6-O** and **P7-O**), while absolute M_w 's of the products by SEC-MALLS is in good agreement with those of the precursors ($M_{w,O}$) (Table 3, $M_w = 132000$ (**S6**), 118000 (**S7**)); the ratio of M_w to $M_{w,O}$ [$M_w/M_{w,O}$] was thus close to 1. These results demonstrate that **P6-O** and **P7-O** are intramolecularly fixed to give single-chain crosslinked star polymers (**S6** and **S7**) with lots of short PEG arms (140-160). It should be noted that this synthetic strategy allows us to precisely and directly control the primary structure (e.g., molecular weight, monomer composition) of single-chain crosslinked star polymers by using olefin-bearing copolymers.

Figure 3

The compactness was further evaluated with the ratio of SEC peak-top molecular weight of **S6**, **S7** (M_p) and that of corresponding precursors ($M_{p,0}$: **P6-O**, **P7-O**) (Table 3, Figure 3a, 3c). The ratio ($M_p/M_{p,0}$) indicates shrinking index of products against precursors. $M_p/M_{p,0}$ for **S6** (0.72) was smaller than that for **S7** (0.87), meaning that **S6** turned more compact against a precursor than **S7**. This is because **P6-O** has fully mobile pendant olefins in high concentration to be efficiently crosslinked into **S6**. Selective single-chain crosslinking of **P7-O** in water was achieved even in the high concentration (up to 80 mg/mL). Analyzed by DLS, R_h of **S7** in CH_2Cl_2 (6.7 nm) was close to that of **P7-O** in D_2O (6.4 nm). This importantly demonstrates that **S7** is effectively crosslinked to maintain the compact self-folding structure in CH_2Cl_2 .

Beyond our anticipation, even in toluene (good solvent), **P6-O** and **P7-O** never induced gelation with dimethyl 2,2'-azobis(2-methylpropionate) (MAIB) under UV irradiation (375 nm) at 25 °C ($[\text{polymer}]_0 = 10 \text{ mg/mL}$). The pendant olefins of **P6-O** and **P7-O** homogeneously consumed up to 86% and 69% conversion in 12 h, respectively. However, the SEC peaks of the products were identical to those of **P6-O** or **P7-O** (Figure 3b, 3d), indicating that the products still maintain the random-coil structure close to the precursors. The unique phenomena propose that, in good solvent, the pendant olefins should be mainly consumed via the addition of a MAIB fragment radical and the subsequent coupling between the adduct radical and a MAIB fragment radical. Such homogeneous reaction in toluene further supports that the selective crosslinking of single chains in water is attributed to not only intramolecular hydrophobic interaction in water but also the steric hindrance of PEG chains that effectively isolate polymer chains.

S6 was further analyzed by transmission electron microscopy (TEM) (Figure 4). The negatively stained micrograph of **S6**, cast on a carbon-coated Cu grid from the aqueous solution, exhibited small white dots below 10 nm without any large aggregates. Thus, selective intramolecular crosslinking of **P6-O** was also visibly confirmed.

Figure 4

Living radical crosslinking. As an alternative of a free radical initiator, a hydrophilic ruthenium catalyst $[\text{RuCp}^*\text{Cl}(\text{PPh}_2(\text{C}_6\text{H}_4\text{OH}))_2]$ was combined with olefin-bearing precursors (**P1-O** – **P5-O**) in water. In this system, the terminal halogens ($\sim\text{C-Br}$) of the self-folding precursors could be reversibly activated by the ruthenium catalyst (Ru) to generate carbon radicals ($\sim\text{C}\cdot + \text{Br-Ru}$) that induce the intramolecular crosslinking through the pendant olefins. The

ruthenium complex was prepared by mixing $[\text{RuCp}^*\text{Cl}]_4$ and $\text{PPh}_2(\text{C}_6\text{H}_4\text{OH})$ in toluene at 80 °C for 12 h. After evaporation, the crude ruthenium was directly utilized for **P1-O** – **P5-O** in water/methanol (9/1, v/v) at 25 °C ($[\text{polymer}]_0 = 5$ or 20 mg/mL).

P1-O – **P5-O** were homogeneously crosslinked without any gelation to give **S1** – **S5** with narrow molecular weight distribution ($M_w/M_n = 1.2 - 1.3$) and molecular weight (M_n, M_p) smaller than the corresponding precursors (Figure 5, Table 3). Crosslinking efficiency (olefin conversion), association number of precursor chains in products (intra- or inter-molecular linking), and compactness of products against precursors were dependent on the following factors: the number of bromine terminals (initiator: **1**, **2**, **3**); olefin content (n); and hydrophobic monomer content ($m + n$).

Figure 5

Owing to low radical concentration via the reversible activation of the carbon-bromine terminus, a ruthenium catalyst induced the crosslinking of **P1-O** – **P5-O** (120 – 360 h) much slower than a free radical initiator for **P6-O** and **P7-O** (16 – 72 h, Table 3). However, the pendant olefins of **P2-O** – **P5-O** with bifunctional and trifunctional initiators (**2**, **3**) were efficiently consumed up to 63 – 70 %, while those of **P1-O** with a monofunctional **1** were consumed up to ~30%.

To estimate the association numbers of polymer chains, final products (**S1-S3**, **S5**) were analyzed by SEC-MALLS (Table 3). **P1-O** – **P3-O**, the precursors for **S1** – **S3**, consist of ~40 mol% hydrophobic monomers $[100 \times (m + n)/\text{DP}]$ with ~10 mol% olefin units $(100 \times n/\text{DP})$, whereas **P5-O**, the precursor for **S5**, carries ~50 mol% hydrophobic monomers with ~10 mol% olefin units. Absolute M_w 's for **S1** and **S2** were determined as 128000 and 120000, respectively, which are in good agreement with those for the corresponding precursors ($M_{w,0}$). Thus, **S1** and **S2** are single chain-crosslinked star polymers. This result is fully consistent with the fact that a PEGMA/DMA random copolymer with 40 mol% DMA efficiently self-fold in water.²³ **S3** also mainly consist of unimolecularly crosslinked star polymers of the branched precursor owing to the M_w relatively close to that of **P3-O**. In contrast, M_w for **S5** (296000) was about twice larger than that for **P5-O** (128000), demonstrating that **S5** consists of two polymer chains of **P5-O**. A PEGMA/DMA (100/100) random copolymer with 50 mol% DMA has been already known to form bimolecular association in water.²³ Thus, **P5-O** would also form a bimolecular aggregate in water during the crosslinking process to uniquely yield a double chain-crosslinked star polymer with quite narrow molecular weight distribution (**S5**, $M_w/M_n = 1.15$).

The shrinking process and compactness for products was further assessed with the SEC peak-top molecular weight ratio of products (M_p) and the corresponding precursors ($M_{p,0}$) $[M_p/M_{p,0}]$. Figure 5a,b plots $M_p/M_{p,0}$ for the products (intermediates) obtained from **S1-O** – **P5-O** against

conversion of the pendant olefin. In all cases, $M_p/M_{p,0}$ became small with increasing conversion, indicating that products gradually shrink with crosslinking. $M_p/M_{p,0}$ for **S1-S3** obtained from **P1-O – P3-O** (n : ~10 mol%) was close to about 0.7, whereas $M_p/M_{p,0}$ for **S4** from **P4-O** (n : 33 mol%) finally reached 0.49 much smaller than that for **S2** (Table 3). This is because **P4-O** with large olefin content can be crosslinked more tightly than **P2-O**. Thus, it reveals that compactness of single chain- and unimolecularly crosslinked star polymers (**S1-S4**) is dependent on the olefin content (n) of the precursors in comparative hydrophobicity ($m + n$: 33 – 40%).

Properties and Functions

Mobility. To evaluate the mobility of crosslinked cores, single chain star polymers (**S6, S7**) were analyzed by ^1H NMR spectroscopy in DMF- d_7 and D_2O at 25 °C, compared with PEGMA/DMA (160/40) random copolymer (**Random**)²³ (Figure 6). All of the samples exhibited broader proton signals of hydrophobic methacrylate backbones (**a, b**) and dodecyl pendants (**c, d, e**) in D_2O than in DMF- d_7 . This indicates that these segments are aggregated within their inner compartments via hydrophobic interaction in water to have restricted mobility. In detail, the dodecyl proton signal (**d**) turned broad in this order: **Random** < **S7** < **S6**; the mobility of the hydrophobic compartments thus decreased in that order. **S6** particularly showed quite broad signals not only in D_2O but also in DMF- d_7 (Figure 6e,f). This is because the HDMA linkage efficiently fixed and stabilized the self-folding structure even in good solvent of DMF- d_7 . In contrast, **S7** exhibited dodecyl proton signals (**c, d, e**, Figure 6b) as sharp as **Random** (Figure 6a), which is consistent with the free mobility of the non-crosslinked dodecyl pendants.

Figure 6

Hydrophobicity. Solvatochromism is effective to evaluate the polarity of the microenvironments of polymeric materials and aggregates. A pyridinium *N*-phenolate betaine dye, so called, Reichardt's dye (**RD**), is well known to show negative solvatochromic shift (blue shift) of UV-vis absorption originating from the intramolecular charge transfer with increasing solvent polarity.^{23,24,39} Actually, the maximum wavelength (λ_{max}) of **RD** shifted to 455 nm in H_2O /acetone (19/1, v/v) from 675 nm in acetone (Figure 7a).

Thus, hydrophobicity of single-chain crosslinked star polymers was evaluated by UV-vis measurements of the aqueous solution of **RD** with **S6** or **S7** in H_2O /acetone (19/1, v/v). To investigate effects of crosslinking on hydrophobicity, **S6** and **S7** were compared with a non-crosslinked **P7-O** (precursor for **S7**); all of the samples contain ~20 mol% of a hydrophobic monomer (HDMA or DMA).

S6, **S7**, and **P7-O** induced negative solvatochromic shift of **RD** more effectively than PPEGMA (homopolymer) and had almost identical λ_{\max} of 545 nm ($[\text{polymer}]_0/[\text{RD}]_0 = 0.045/0.45$ mM) (Figure 7). This means that **RD** was encapsulated into the crosslinked or self-folding compartments to give UV-vis absorptions reflecting the hydrophobic micro-domains. Importantly, hydrophobicity of polymer compartments is just dependent on the hydrophobic monomer content and independent of the mobility. However, in contrast to a non-crosslinked **P7-O**, **S6** and **S7** effectively induced the blue shift of **RD** even in a small feed of the polymers against **RD** [$\lambda_{\max} = 536$ (**S6**), 524 (**S7**), and 485 (**P7-O**) nm, $[\text{polymer}]_0/[\text{RD}]_0 = 0.0045/0.45$ mM]. This importantly demonstrates that single-chain crosslinked star polymers (**S6** and **S7**) enclose a hydrophobic **RD** within the fixed compartments more efficiently and stably than a non-crosslinked counterpart.

Figure 7

Thermosensitive Solubility. PEG and the related materials often show thermosensitive solubility in water to induce lower critical solution temperature (LCST)-type phase separation upon heating.^{7,11,23,24,40} Thus, cloud point (Cp) of an olefin-bearing precursor (**P1-O**) and the crosslinked star polymer (**S1**) was determined by UV-vis measurements of their aqueous solutions scanning from 70 °C to 95 °C with the heating rate of 1 °C/min ($[\text{polymer}] = 4$ mg/mL). As shown in Figure 8, both of the solutions turned turbid upon heating. However, the Cp of **S1** (~81 °C; ~90% transmittance) was clearly higher than the Cp of **P1-O** (~76 °C; ~90% transmittance) despite of the perfectly identical composition of their polymers. The unique phenomenon is probably because hydrophobic dodecyl pendants in **S1** are stably confined within the crosslinked inner core to hardly promote the dehydration of PEG chains.

Figure 8

Conclusion

In conclusion, we successfully produced single chain-crosslinked star polymers as a new class of star polymers via the intramolecular crosslinking of self-folding amphiphilic copolymers in water. For this, amphiphilic random copolymers carrying hydrophilic PEG chains and hydrophobic dodecyl and olefin pendants were synthesized via ruthenium-catalyzed living radical polymerization of PEGMA, DMA, and HDMA or HEMA, and the in-situ or post-esterification of the resulting hydroxyl-functionalized copolymers with methacryloyl chloride. Olefin-bearing precursors with 20 – 40 mol% hydrophobic units efficiently self-folded in water via hydrophobic interaction to form unimer micelles placing olefin pendants within the inner cores. The

self-folding precursors were thus intramolecularly crosslinked with a free radical initiator or a ruthenium catalyst in water to give single chain-crosslinked star polymers. In contrast, an olefin-bearing precursor with 50 mol% hydrophobic units gave double chain-crosslinked star polymers via the bimolecular association of the precursor in water. Primary structure of these star polymers can be precisely controlled with amphiphilic random copolymer precursors. Thus, the star polymers developed herein would be promising as scaffolds for novel functional macromolecules and precision nanospaces.

Acknowledgment

This research was supported by the Ministry of Education, Science, Sports and Culture through Grant-in-Aids for Scientific Research (A: 24245026, C: 26410134) and Young Scientist (B: 24750104). We also thank Mr. Akihiro Uesaka and Prof. Syunsaku Kimura (Department of Material Chemistry, Kyoto University) for TEM measurements.

References

- (1) Terashima, T. Functional spaces in star and single-chain polymers via living radical polymerization. *Polym. J.* **46**, 664-673 (2014).
- (2) Terashima, T. & Sawamoto, M. Microgel-core star polymers as functional compartments for catalysis and molecular recognition. *ACS Symp. Ser.* **1101**, 65-80 (2012).
- (3) Blencowe, A., Tan, J. F., Goh, T. K. & Qiao, G. G. Core cross-linked star polymers via controlled radical polymerisation. *Polymer* **50**, 5-32 (2009).
- (4) Gao, H. Development of star polymers as unimolecular containers for nanomaterials. *Macromol. Rapid Commun.* **33**, 722-734 (2012).
- (5) Elsabahy, M. & Wooley, K. L. Strategies toward well-defined polymer nanoparticles inspired by nature: chemistry versus versatility. *J. Polym. Sci. Part A: Polym. Chem.* **50**, 1869-1880 (2012).
- (6) Terashima, T., Motokawa, R., Koizumi, S., Sawamoto, M., Kamigaito, M., Ando, T. & Hashimoto, T. In situ and time-resolved small-angle neutron scattering observation of star polymer formation via arm-linking reaction in ruthenium-catalyzed living radical polymerization. *Macromolecules* **43**, 8218-8232 (2010).
- (7) Terashima, T., Nishioka, S., Koda, Y., Takenaka, M. & Sawamoto, M. Arm-cleavable microgel star polymers: a versatile strategy for direct core analysis and functionalization. *J. Am. Chem. Soc.* **136**, 10254-10257 (2014).

- (8) Terashima, T., Ouchi, M., Ando, T. & Sawamoto, M. Transfer hydrogenation of ketones catalyzed by PEG-armed ruthenium-microgel star polymers: microgel-core reaction space for active, versatile and recyclable catalysis. *Polym. J.* **43**, 770-777 (2011).
- (9) Terashima, T., Nomura, A., Ito, M., Ouchi, M. & Sawamoto, M. Star-polymer-catalyzed living radical polymerization: microgel-core reaction vessel by tandem catalyst interchange. *Angew. Chem. Int. Ed.* **50**, 7892-7895 (2011).
- (10) Chi, Y., Scroggins, S. T. & Fréchet, J. M. J. One-pot multi-component asymmetric cascade reactions catalyzed by soluble star polymers with highly branched non-interpenetrating catalytic cores. *J. Am. Chem. Soc.* **130**, 6322-6323 (2008).
- (11) Kanaoka, S., Yagi, N., Fukuyama, Y., Aoshima, S., Tsunoyama, H., Tsukuda, T. & Sakurai, H. Thermosensitive gold nanoclusters stabilized by well-defined vinyl ether star polymers: reusable and durable catalysts for aerobic alcohol oxidation. *J. Am. Chem. Soc.* **129**, 12060-12061 (2007).
- (12) Koda, Y., Terashima, T. & Sawamoto, M. Fluorous microgel star polymers: selective recognition and separation of polyfluorinated surfactants and compounds in water. *J. Am. Chem. Soc.* **136**, 15742-15748 (2014).
- (13) Ouchi, M., Terashima, T. & Sawamoto, M. Transition metal-catalyzed living radical polymerization: toward perfection in catalysis and precision polymer synthesis. *Chem. Rev.* **109**, 4963-5050 (2009).
- (14) Ouchi, M., Badi, N., Lutz, J.-F. & Sawamoto, M. Single-chain technology using discrete synthetic macromolecules. *Nat. Chem.* **3**, 917-924 (2011).
- (15) Altintas, O. & Barner-Kowollik, C. Single-chain folding of synthetic polymers by covalent and non-covalent interactions: current status and future perspectives. *Macromol. Rapid Commun.* **33**, 958-971 (2012).
- (16) Sanchez-sanchez, A., Pérez-Baena, I. & Pomposo, J. A. Advances in click chemistry for single-chain nanoparticle construction. *Molecules* **18**, 3339-3355 (2013).
- (17) Terashima, T. & Sawamoto, M. Sequence-regulated polymers via living radical polymerization: from design to properties and functions. *ACS Symp. Ser.* **1170**, 255-267 (2014).
- (18) Artar, M., Huerta, E., Meijer, E. W. & Palmans, A. R. A. Dynamic single chain polymeric nanoparticles: from structure to functions. *ACS Symp. Ser.* **1170**, 313-325 (2014).
- (19) Li, L., Raghupathi, K., Song, C., Prasad, P. & Thayumanavan, S. Self-assembly of random copolymers. *Chem. Commun.* **50**, 13417-13432 (2014).
- (20) Lyon, C. K., Prasher, A., Hanlon, A. M., Tuten, B. T., Tooley, C. A., Frank, P. G. & Berda, E. B. A brief user's guide to single-chain nanoparticles. *Polym. Chem.* **6**, 181-197 (2015).

- (21) Morishima, Y., Nomura, S., Ikeda, T., Seki, M. & Kamachi, M. Characterization of unimolecular micelles of random copolymers of sodium 2-(acrylamide)-2-methylpropanesulfonate and methacrylamides bearing bulky hydrophobic substituents. *Macromolecules* **28**, 2874-2881 (1995).
- (22) Yusa, S., Sakakibara, S., Yamamoto, T. & Morishima, Y. Fluorescence studies of pH-responsive unimolecular micelles formed from amphiphilic polysulfonates possessing long-chain alkyl carboxyl pendants. *Macromolecules* **35**, 10182-10188 (2002).
- (23) Terashima, T., Sugita, T., Fukae, K. & Sawamoto, M. Synthesis and single-chain folding of amphiphilic random copolymers in water. *Macromolecules* **47**, 589-600 (2014).
- (24) Sugita, T., Matsumoto, K., Terashima, T. & Sawamoto, M. Synthesis of amphiphilic three-armed star random copolymers via living radical polymerization and their unimolecular folding properties in water. *Macromol. Symp.* **350**, 76-85 (2015)
- (25) Terashima, T., Mes, T., de Greef, T. F. A., Gillissen, M. A. J., Besenius, P., Palmans, A. R. A. & Meijer, E. W. Single-chain folding of polymers for catalytic systems in water. *J. Am. Chem. Soc.* **133**, 4742-4745 (2011).
- (26) Gillissen, M. A. J., Terashima, T., Meijer, E. W., Palmans, A. R. A. & Voets, I. K. Sticky supramolecular grafts stretch single polymer chains. *Macromolecules* **46**, 4120-4125 (2013).
- (27) Arter, M., Terashima, T., Sawamoto, M., Meijer, E. W. & Palmans, A. R. A. Understanding the catalytic activity of single-chain polymeric nanoparticles in water. *J. Polym. Sci. Part A: Polym. Chem.* **52**, 12-20 (2014).
- (28) Foster, E. J., Berda, E. B. & Meijer, E. W. Metastable supramolecular polymer nanoparticles via intramolecular collapse of single polymer chains. *J. Am. Chem. Soc.* **131**, 6964-6966 (2009).
- (29) Mes, T., van der Weegen, R., Palmans, A. R. A. & Meijer, E. W. Single-chain polymeric nanoparticles by stepwise folding. *Angew. Chem. Int. Ed.* **50**, 5085-5089 (2011).
- (30) Hosono, N., Gillissen, M. A. J., Li, Y., Sheiko, S. S., Palmans, A. R. A. & Meijer, E. W. orthogonal self-assembly in folding block copolymers. *J. Am. Chem. Soc.* **135**, 501-510 (2013).
- (31) Altintas, O., Lejeune, E., Gerstel, P. & Barner-Kowollik, C. Bioinspired dual self-folding of single polymer chains via reversible hydrogen bonding. *Polym. Chem.* **3**, 640-651 (2012).
- (32) Croce, T. A.; Hamilton, S. K.; Chen, M. L.; Muchalski, H.; Harth, E. *Macromolecules* **2007**, *40*, 6028-6031.
- (33) Cherian, A. E., Sun, F. C., Sheiko, S. S. & Coates, G. W. Formation of nanoparticles by intramolecular cross-linking: following the reaction process of single polymer chains by atomic force microscopy. *J. Am. Chem. Soc.* **129**, 11350-11351 (2007).

- (34) Murray, B. S. & Fulton, D. A. Dynamic covalent single-chain polymer nanoparticles. *Macromolecules* **44**, 7242-7252 (2011).
- (35) Chao, D., Jia, X., Tuten, B., Wang, C. & Berda, E. B. Controlled folding of a novel electroactive polyolefin via multiple sequential orthogonal intra-chain interactions. *Chem. Commun.* **49**, 4178-4180 (2013).
- (36) Ouchi, M., Yoda, H., Terashima, T. & Sawamoto, M. Aqueous metal-catalyzed living radical polymerization: highly active water-assisted catalysis. *Polym. J.* **44**, 51-58 (2012).
- (37) Ouchi, M., Ito, M., Kamemoto, S. & Sawamoto, M. Highly active and removable ruthenium catalysts for transition-metal-catalyzed living radical polymerization: design of ligands and cocatalysts. *Chem. Asian J.* **3**, 1358-1364 (2008).
- (38) Yoda, H., Nakatani, K., Terashima, T., Ouchi, M. & Sawamoto, M. Ethanol-mediated living radical homo- and copolymerizations with Cp*-ruthenium catalysts: active, robust, and universal for functionalized methacrylates. *Macromolecules* **43**, 5595-5601 (2010).
- (39) Reichardt, C. Solvatochromic dyes as solvent polarity indicators. *Chem. Rev.* **94**, 2319-2358 (1994).
- (40) Lutz, J.-F. Polymerization of oligo(ethylene glycol) (meth)acrylates: toward new generations of smart biocompatible materials. *J. Polym. Sci. Part A: Polym. Chem.* **46**, 3459-3470 (2008).

Figure Legend

Scheme 1. (a) Synthesis of olefin-bearing amphiphilic random copolymers (**P1-O** – **P7-O**) via ruthenium-catalyzed living radical polymerization of PEGMA, DMA, and HDMA or HEMA with **1** – **4**, followed by the esterification of hydroxyl-functionalized amphiphilic random copolymers (**P1** – **P7**) with methacryloyl chloride. (b) Synthesis of single-chain crosslinked star polymers (**S1** – **S7**) via the intramolecular crosslinking of self-folding precursors (**P1-O** – **P7-O**) with an azo initiator or a ruthenium catalyst in water.

Figure 1. Synthesis of hydroxyl-functionalized amphiphilic copolymers (**P2**, **P3**, **P6**, **P7**) via ruthenium-catalyzed living radical polymerization of PEGMA, DMA, and HDMA or HEMA with **2** (**P2**: a, e), **3** (**P3**: b, f), and **4** (**P6**: c, g; **P7**: d, h): (a-d) time-conversion curves and (e-h) SEC curves. (e-h) Esterification of the hydroxyl groups of **P2**, **P3**, **P6**, and **P7** with methacryloyl chloride into olefin-bearing amphiphilic copolymers (e: **P2-O**, f: **P3-O**, g: **P6-O**, h: **P7-O**).

Figure 2. ^1H NMR spectra of (a) **P1**, (b) **P1-O**, (c) **P2-O**, and (d) **P7-O** in acetone- d_6 (a-c) or methanol- d_4 (d) at 25 °C.

Figure 3. Synthesis of single-chain crosslinked star polymers (solid lines) via the intramolecular crosslinking of (a, b) **P6-O** or (c, d) **P7-O** with (a, c) V-50 in water or (b, d) MAIB in toluene at 25 °C under UV irradiation (375 nm): [olefin in precursor] $_0$ = 4.2 (**P6-O**), 1.1 (**P7-O**) mM, [V-50] $_0$ = 3.7 mM, [MAIB] $_0$ = 4.3 mM ([polymer] $_0$ /[initiator] $_0$ = 10/1.0 mg/mL).

Figure 4. Transmission electron micrograph of **S6** cast from the aqueous solution ([**S6**] = 1.0×10^{-4} g/L). The sample is negatively stained with 2% uranyl acetate (white dots: **S6**; black: background).

Figure 5. Synthesis of star polymers via the intramolecular crosslinking of **P1-O**, **P2-O**, **P3-O**, **P4-O**, and **P5-O** with a ruthenium catalyst in water: [olefin in precursor] $_0$ /[RuCp*Cl(PPh $_2$ (C $_6$ H $_4$ OH)) $_2$] $_0$ = 1.0/0.2 (**S1-S3**), 4.0/0.8 (**S4**, **S5**) mM in H $_2$ O/ethanol (9/1, v/v) at 25 °C.

Figure 6. ^1H NMR spectra of (a, b) PEGMA/DMA (160/40) random copolymer (**Random**), (c, d) **S7**, and (e, f) **S6** in DMF- d_7 (a, c, e) and D $_2$ O (b, d, f) at 25 °C.

Figure 7. (a) UV-vis spectra of Reichardt's dye (**RD**) (long dash), **RD** with **S7** (black), and **RD** with **P7-O** (gray) in H₂O/acetone (19/1, v/v) and **RD** in acetone (dash) at 25 °C: [polymer]₀/[**RD**]₀ = 0.045/0.45 mM. (b) Effects of polymer concentration (**S6**: filled square; **S7**: open square; **P7-O**: filled circle; PPEGMA: open circle) on λ_{\max} of **RD**: [polymer]₀/[**RD**]₀ = 0.0045/0.45 – 0.090/0.45 mM in H₂O/acetone (19/1, v/v) at 25 °C.

Figure 8. Transmittance of the aqueous solutions of **P1-O** and **S1** as a function of temperature (heating rate and range: 1 °C/min from 70 to 95 °C): [polymer] = 4 mg/mL.

Table 1. Hydroxyl-Functionalized Amphiphilic Random Copolymers via Living Radical Polymerization^a

code	initiator	monomer	$l/m/n_{\text{calcd}}$ ^b	time (h)	conv. (%) ^c (PEGMA/(H)DMA/HEMA)	M_n^d	M_w/M_n^d
P1	1	PEGMA/DMA/HDMA	120/60/20	61	79/86	63800	1.32
P2	2	PEGMA/DMA/HDMA	150/75/25	25	80/80	50300	1.40
P3	3	PEGMA/DMA/HDMA	150/75/25	25	91/91	47400	1.32
P4	2	PEGMA/HDMA	150/0/100	29	77/79	73600	1.42
P5	2	PEGMA/DMA/HDMA	125/100/25	29	93/93	55900	1.45
P6	4	PEGMA/HDMA	200/0/50	28	77/79	58500	1.35
P7	4	PEGMA/DMA/HEMA	200/50/13	47	74/78/80	57000	1.20

^a**P1**: [PEGMA]₀/[DMA]₀/[HDMA]₀/[**1**]₀/[RuCp*Cl(PPh₃)₂]₀/[4-DMAB]₀ = 500/250/83/4.2/0.4/40 mM in ethanol at 40 °C; **P2**, **P3**: [PEGMA]₀/[DMA]₀/[HDMA]₀/[**2** or **3**]₀/[Ru(Ind)Cl(PPh₃)₂]₀/[*n*-Bu₃N]₀ = 300/150/50/2/1.0/20 mM in THF at 60 °C; **P4**, **P5**: [PEGMA]₀/[DMA]₀/[HDMA]₀/[**2**]₀/[Ru(Ind)Cl(PPh₃)₂]₀/[*n*-Bu₃N]₀ = 300/0/200/2/0.4/4 (**P4**), 300/240/60/2.4/0.5/5 (**P5**) mM in THF at 60 °C; **P6**: [PEGMA]₀/[HDMA]₀/[**4**]₀/[Ru(Ind)Cl(PPh₃)₂]₀/[*n*-Bu₃N]₀ = 400/100/2/0.5/10 mM in toluene at 80 °C; **P7**: [PEGMA]₀/[DMA]₀/[HEMA]₀/[**4**]₀/[RuCp*Cl(PPh₃)₂]₀/[4-DMAB]₀ = 400/100/25/2.0/0.2/20 mM in ethanol at 40 °C.

^b l = [PEGMA]₀/[initiator]₀, m = [DMA]₀/[initiator]₀, n = [HDMA or HEMA]₀/[initiator]₀.

^cMonomer conversion determined by ¹H NMR. (H)DMA = total conversion of HDMA and DMA.

^dDetermined by SEC in DMF (10 mM LiBr) with PMMA calibration.

Table 2. Characterization of Olefin-Bearing Amphiphilic Copolymers^a

code	precursor	$l/m/n_{\text{DP}}$ ($l/m/n_{\text{ratio}}$) ^b	M_n^c	M_w/M_n^c	$M_{p,O}^c$	M_n^b (NMR)	$M_{w,O}^d$ (MALLS)
P1-O	P1	(120/61/14)	63300	1.34	85600	-	129000
P2-O	P2	157/76/23	58500	1.27	71900	102000	126000
P3-O	P3	(150/71/20)	50400	1.28	63200	-	112000
P4-O	P4	166/0/81	74300	1.33	96600	107000	160000
P5-O	P5	140/113/23	57500	1.36	75600	103000	128000
P6-O	P6	163/0/38	61900	1.32	75400	90500	131000
P7-O	P7	141/35/8.3	58800	1.18	69100	77700	109000

^a**P1-O**, **P6-O**, and **P7-O**: Post-esterification of the OH groups of isolated **P1**, **P6**, and **P7** with methacryloyl chloride (MAC) ([OH]/[MAC] = 1/5) in THF. **P2-O-P5-O**: In situ esterification of the OH groups of **P2-P5** via the direct addition of MAC into the polymerization solutions ([OH]/[MAC] = 1/5).

^bMonomer composition ($l/m/n_{\text{DP}}$: degree of polymerization; $l/m/n_{\text{ratio}}$: ratio) determined by ¹H NMR.

^cDetermined by SEC in DMF (10 mM LiBr) with PMMA calibration.

^dDetermined by SEC-MALLS in DMF (10 mM LiBr).

Table 3. Characterization of Star Polymers^a

code	precursor	m/n ($m+n$) (mol %)	[precursor] ₀ (mg/mL)	time (h)	conv. ^b (%)	M_n^c	M_w/M_n^c	M_p^c	$M_p/M_{p,O}^d$	M_w^e (MALLS)	$M_w/M_{w,O}^f$
S1	P1-O	31/7 (38)	5	360	31	50400	1.29	62500	0.73	128000	0.99
S2	P2-O	30/9 (39)	5	120	63	48900	1.22	47900	0.64	120000	0.95
S3	P3-O	30/8 (38)	5	120	70	45900	1.23	47300	0.75	166000	1.5
S4	P4-O	- /33 (33)	5	120	66	48200	1.24	47600	0.49	-	-
S5	P5-O	41/8 (49)	20	120	65	58500	1.15	59300	0.78	296000	2.3
S6	P6-O	- /19 (19)	10	16	89	44300	1.31	55800	0.74	132000	1.0
S7	P7-O	19/5 (24)	10	72	77	50200	1.23	60000	0.87	118000	1.1

^a**S1 – S5**: [Olefin in precursor]₀/[RuCp*Cl(PPh₂(C₆H₄OH))₂]₀ = 1.0/0.2 (**S1-S3**), 4.0/0.8 (**S4, S5**) mM in H₂O/ethanol (9/1, v/v) at 25 °C ([precursor]₀ = 5 (**P1-O – P4-O**), 20 (**P5-O**) mg/mL). **S6, S7**: [olefin in precursor]₀/[V-50]₀ = 4.2/3.7 (**S6**), 1.1/3.7 (**S7**) mM in H₂O at 25 °C under UV irradiation (375 nm) ([precursor]₀ = 10 mg/mL).

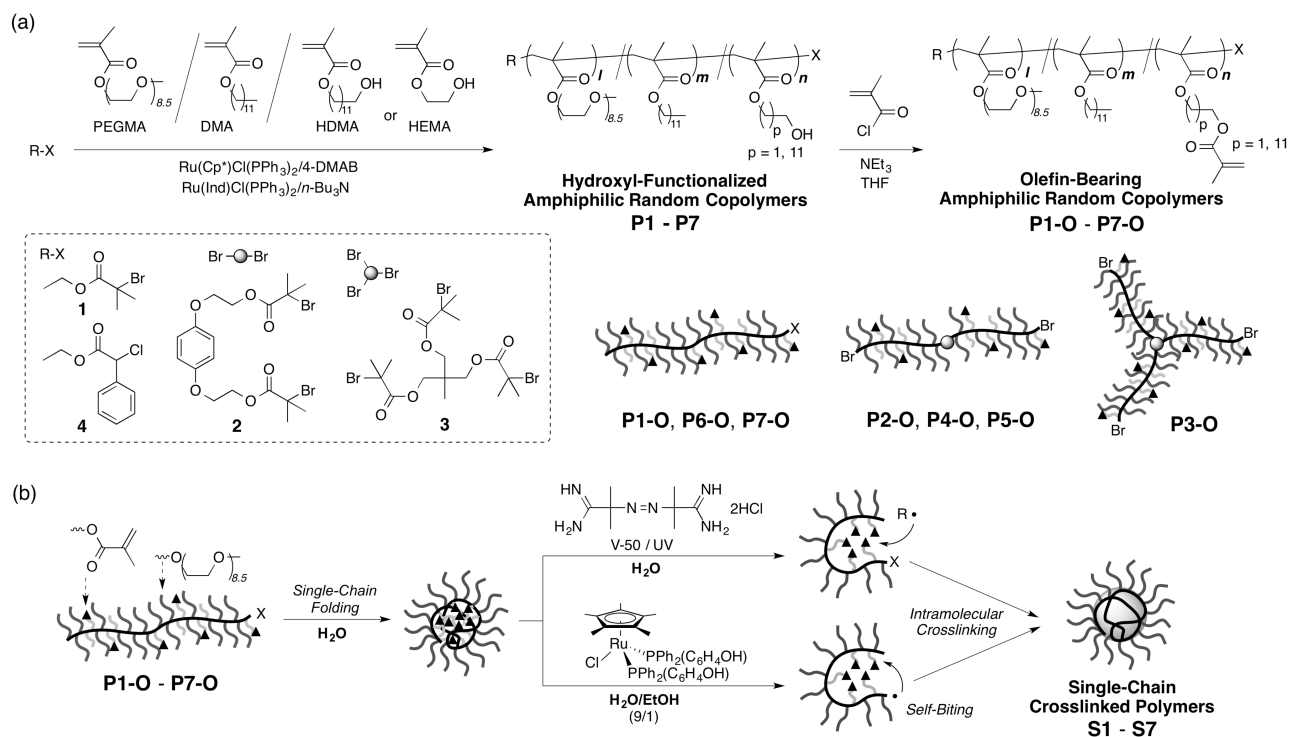
^bConversion of pendant olefin determined by ¹H NMR.

^cDetermined by SEC in DMF (10 mM LiBr) with PMMA calibration.

^d $M_{p,O}$: peak top molecular weight of **PO-1 – PO-7** (see Table 2).

^eAbsolute weight-average molecular weight determined by SEC-MALLS in DMF (10 mM LiBr).

^f $M_w/M_{w,O}$: Aggregation number of **PO-1 – PO-7** in **S1 – S7**. $M_{w,O}$: Absolute weight-average molecular weight of **PO-1 – PO-7**.



Scheme 1. (a) Synthesis of olefin-bearing amphiphilic random copolymers (**P1-O – P7-O**) via ruthenium-catalyzed living radical polymerization of PEGMA, DMA, and HDMA or HEMA with **1 – 4**, followed by the esterification of hydroxyl-functionalized amphiphilic random copolymers (**P1 – P7**) with methacryloyl chloride. (b) Synthesis of single-chain crosslinked star polymers (**S1 – S7**) via the intramolecular crosslinking of self-folding precursors (**P1-O – P7-O**) with an azo initiator or a ruthenium catalyst in water.

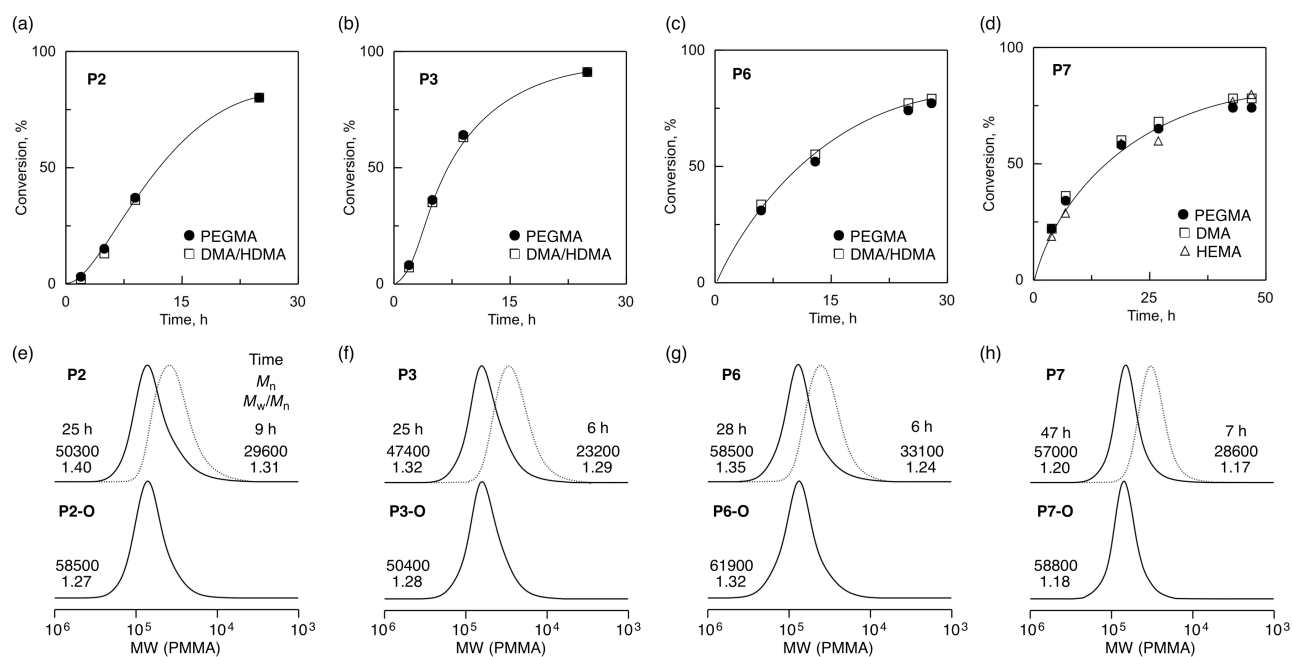


Figure 1. Synthesis of hydroxyl-functionalized amphiphilic copolymers (**P2**, **P3**, **P6**, **P7**) via ruthenium-catalyzed living radical polymerization of PEGMA, DMA, and HDMA or HEMA with **2** (**P2**: a, e), **3** (**P3**: b, f), and **4** (**P6**: c, g; **P7**: d, h): (a-d) time-conversion curves and (e-h) SEC curves. (e-h) Esterification of the hydroxyl groups of **P2**, **P3**, **P6**, and **P7** with methacryloyl chloride into olefin-bearing amphiphilic copolymers (e: **P2-O**, f: **P3-O**, g: **P6-O**, h: **P7-O**).

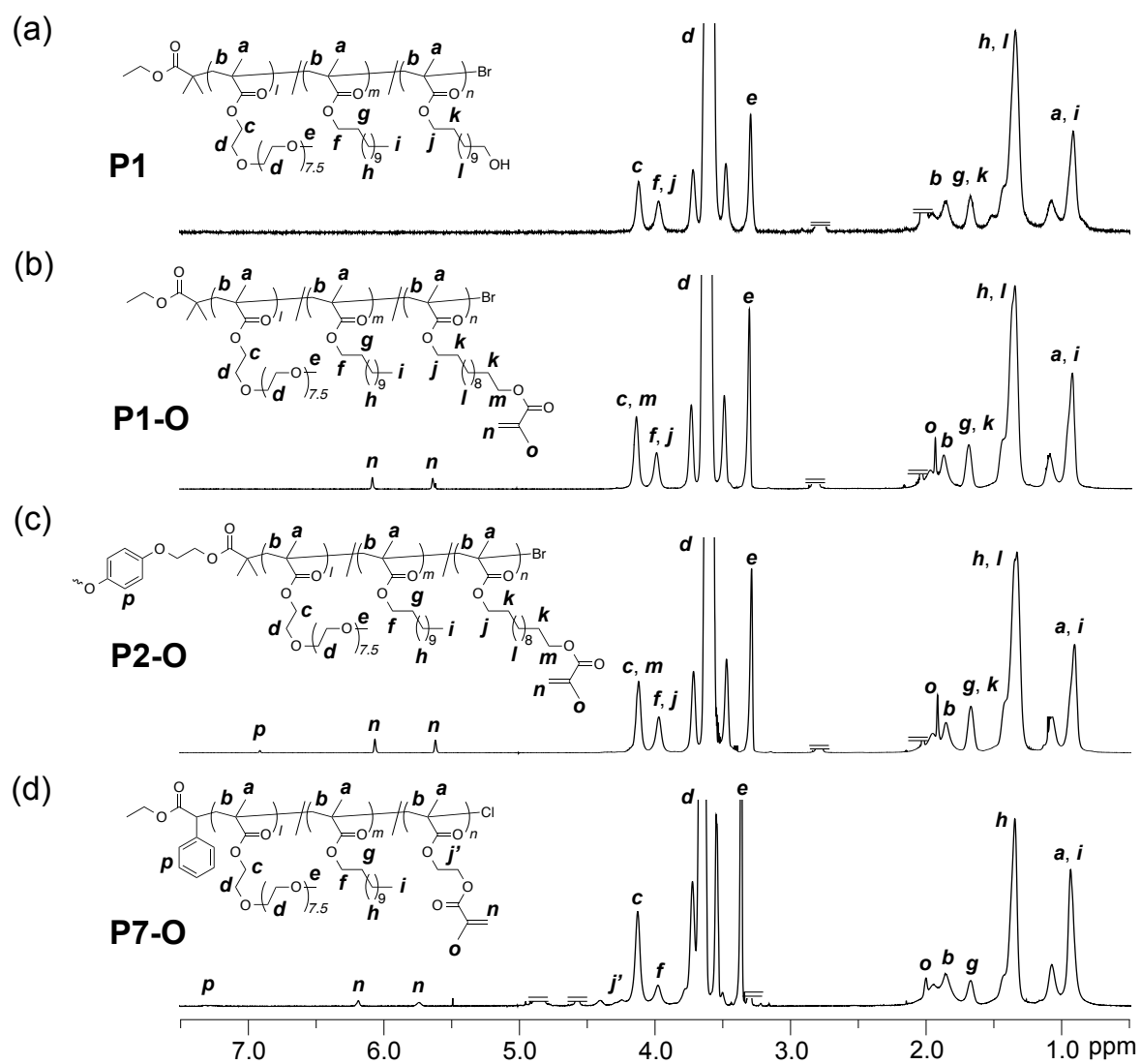


Figure 2. ^1H NMR spectra of (a) **P1**, (b) **P1-O**, (c) **P2-O**, and (d) **P7-O** in acetone- d_6 (a-c) or methanol- d_4 (d) at 25 °C.

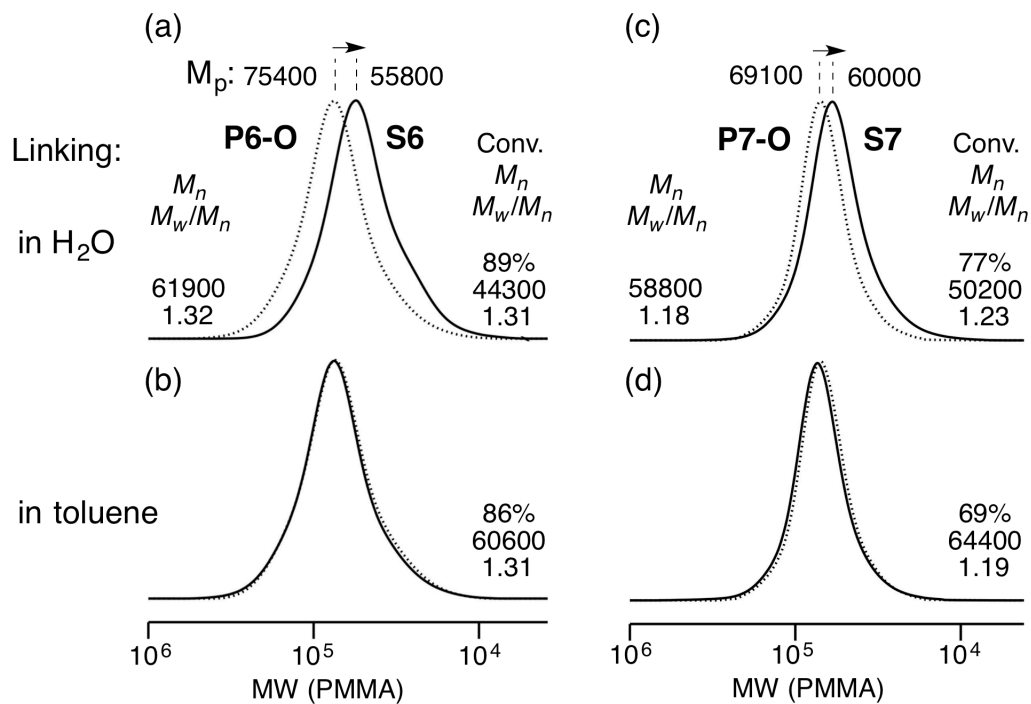


Figure 3. Synthesis of single-chain crosslinked star polymers (solid lines) via the intramolecular crosslinking of (a, b) **P6-O** or (c, d) **P7-O** with (a, c) V-50 in water or (b, d) MAIB in toluene at 25 °C under UV irradiation (375 nm): [olefin in precursor]₀ = 4.2 (**P6-O**), 1.1 (**P7-O**) mM, [V-50]₀ = 3.7 mM, [MAIB]₀ = 4.3 mM ([polymer]₀/[initiator]₀ = 10/1.0 mg/mL).

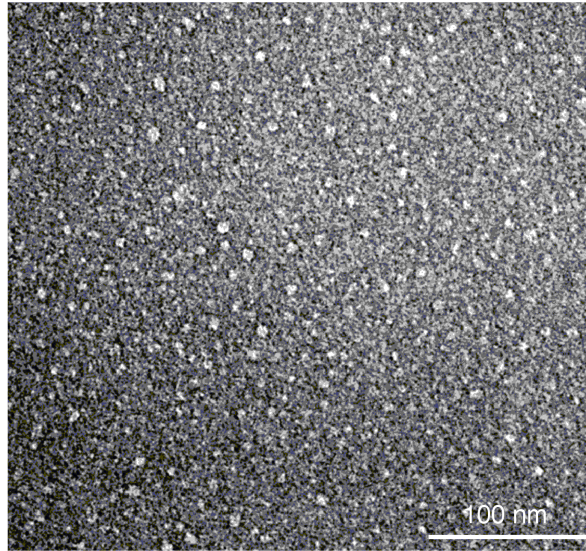


Figure 4. Transmission electron micrograph of **S6** cast from the aqueous solution ($[S6] = 1.0 \times 10^{-4} \text{ g/L}$). The sample is negatively stained with 2% uranyl acetate (white dots: **S6**; black: background).

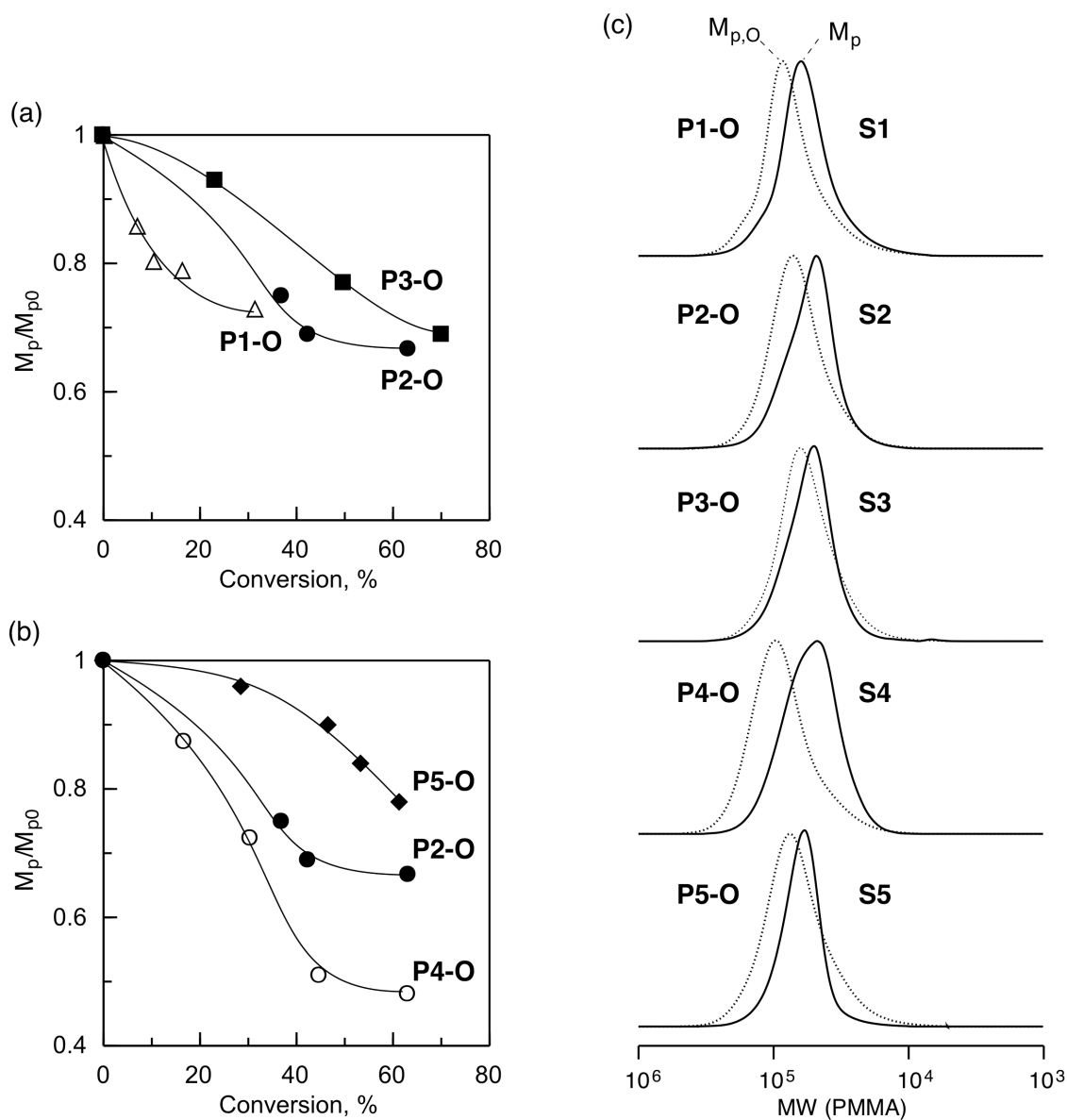


Figure 5. Synthesis of star polymers via the intramolecular crosslinking of **P1-O**, **P2-O**, **P3-O**, **P4-O**, and **P5-O** with a ruthenium catalyst in water: [olefin in precursor]₀/[RuCp*Cl(PPh₂(C₆H₄OH))₂]₀ = 1.0/0.2 (**S1-S3**), 4.0/0.8 (**S4, S5**) mM in H₂O/ethanol (9/1, v/v) at 25 °C.

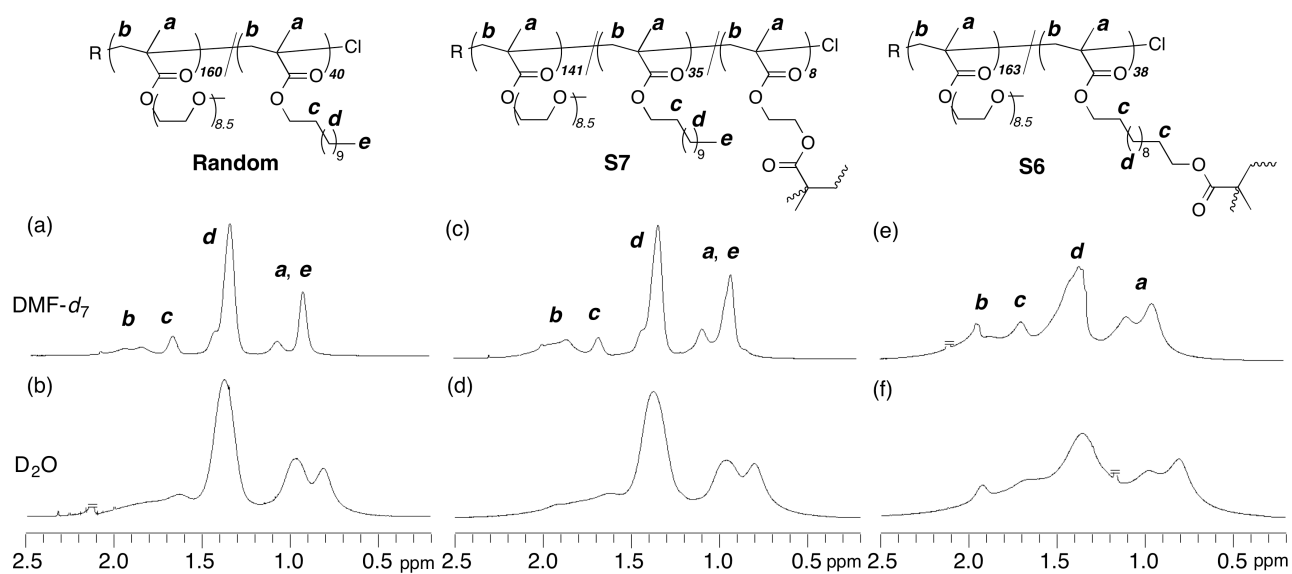


Figure 6. ^1H NMR spectra of (a, b) PEGMA/DMA (160/40) random copolymer (**Random**), (c, d) **S7**, and (e, f) **S6** in $\text{DMF-}d_7$ (a, c, e) and D_2O (b, d, f) at 25 °C.

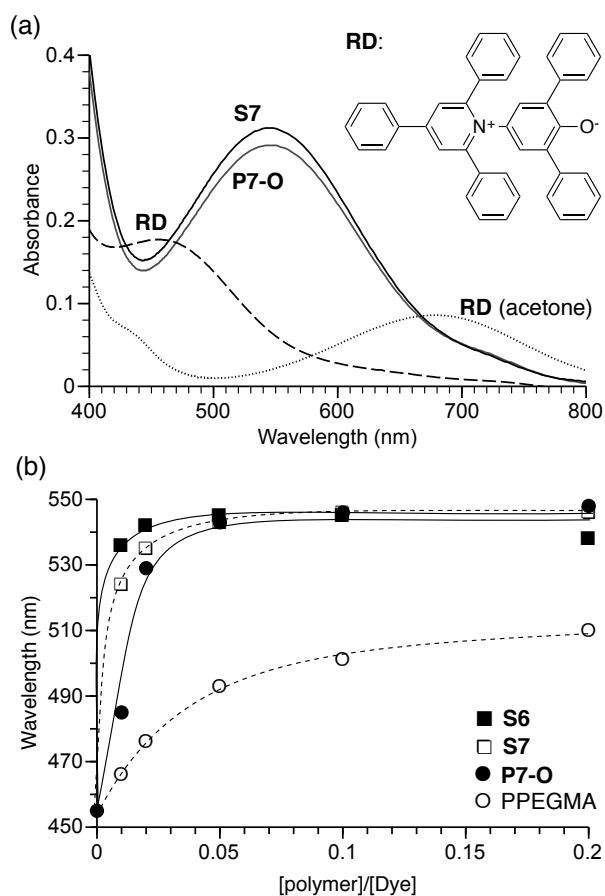


Figure 7. (a) UV-vis spectra of Reichardt's dye (**RD**) (long dash), **RD** with **S7** (black), and **RD** with **P7-O** (gray) in H₂O/acetone (19/1, v/v) and **RD** in acetone (dash) at 25 °C: [polymer]₀/[RD]₀ = 0.045/0.45 mM. (b) Effects of polymer concentration (**S6**: filled square; **S7**: open square; **P7-O**: filled circle; PPEGMA: open circle) on λ_{\max} of **RD**: [polymer]₀/[RD]₀ = 0.0045/0.45 – 0.090/0.45 mM in H₂O/acetone (19/1, v/v) at 25 °C.

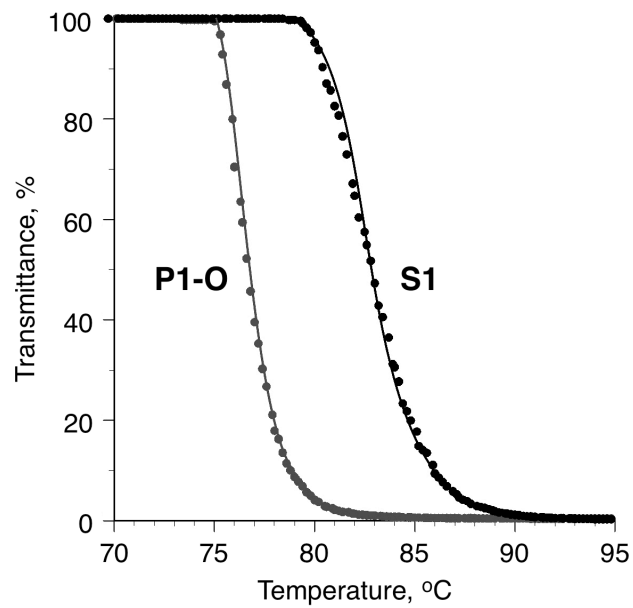


Figure 8. Transmittance of the aqueous solutions of **P1-O** and **S1** as a function of temperature (heating rate and range: 1 °C/min from 70 to 95 °C): [polymer] = 4 mg/mL.